International Journal of Thermophysics, Vol. 7, No. 2, 1986

Determination of Thermal Conductivity from Specific Heat and Thermal Diffusivity Measurements of Plasma-Sprayed Cermets[1]

E. P. Roth[2] and M. F. Smith[2]

The thermal conductivities of three plasma-sprayed cermets have been determined over the temperature range 23–630°C from the measurement of the specific heat, thermal diffusivity, and density. These cermets are mixtures of Al and SiC prepared by plasma spray deposition and are being considered for various applications in magnetic confinement fusion devices. The samples consisted of three compositions: 61 vol% Al/39 vol% SiC, 74 vol% Al/26 vol% SiC, and 83 vol% Al/17 vol% SiC. The specific heat was determined by differential scanning calorimetry through the Al melt transition up to 720°C, while the thermal diffusivity was determined using the laser flash technique up to 630°C. The linear thermal expansion was measured and used to correct the diffusivity and density values. The thermal diffusivity showed a significant increase after thermal cycling due to a reduction in the intergrain contact resistance, increasing from 0.4 to 0.6 $cm^2 \cdot s^{-1}$ at 160°C. However, effective medium theory calculations indicated that the thermal conductivities of both the Al and the SiC were below the ideal defect-free limit even after high-temperature cycling. The specific heat measurements showed suppressed melting points in the plasma-sprayed cermets. The 39 vol% SiC began a melt endotherm at 577°C, which peaked in the 640–650°C range depending on the sample thermal history. Chemical and X-ray diffraction analysis indicated the presence of free silicon in the cermet and in the SiC powder, which resulted in a eutectic Al/Si alloy.

KEY WORDS: aluminium/silicon carbide cermet; aluminum/silicon eutectic; plasma spray; specific heat; thermal conductivity; thermal diffusivity.

[1] Paper presented at the Ninth Symposium on Thermophysical Properties, June 24–27, 1985, Boulder, Colorado, U.S.A.

[2] Sandia National Laboratories, Albuquerque, New Mexico 87185, U.S.A.

0195-928X/86/0300-0455$05.00/0

1. INTRODUCTION

Interior surfaces in magnetic confinement fusion reactors can undergo high rates of erosion due to exposure to high plasma temperatures. Surfaces of low atomic number, Z, are being considered as a thermal armor in future long-pulse machines either as a bonded cladding or as a coating [1]. Cermet coatings, such as aluminum and silicon carbide, can serve as a graded transition between a metal heat sink and a low-Z cladding by providing good thermal contact to the metal heat sink and accommodating the large mismatch in thermal expansion between the heat sink and the cladding. These coatings can also be used as direct thermal barriers by grading the Al/SiC ratio from a metal-rich base to a refractory-rich outer surface.

Plasma spray deposition has been successfully used to form thick coatings of this cermet material over large surfaces. The cermet composition has been varied to try to achieve a mixture with good thermal conductivity, thermal shock resistance, and adhesion.

Three compositions of Al/SiC cermets were prepared for thermal property analysis. The material's specific heat, thermal diffusivity, density, and thermal expansion were measured and used to calculate the thermal conductivity using the expression,

$$\lambda = \alpha \rho c_p \tag{1}$$

where λ is the thermal conductivity ($W \cdot m^{-1} \cdot °C^{-1}$), α is the diffusivity ($m^2 \cdot s^{-1}$), ρ is the density ($g \cdot m^{-3}$), and is the c_p is the specific heat ($J \cdot g^{-1} \cdot °C^{-1}$). This paper describes the thermal behavior of these materials from room temperature up to and, for some samples, through the aluminum melt transition at 660°C. The results of microstructural and compositional analyses are also described.

2. EXPERIMENT

2.1. Sample Preparation

The Al/SiC cermets were prepared by low-pressure chamber plasma spraying [1]. SiC and Al powders were blended and then cosprayed through a single plasma spray gun. The coatings were sprayed on copper blocks and subsequently removed by sawing away the bulk substrate and then acid dissolving the remaining copper.

Three cermet compositions were prepared with SiC contents of 39, 26, and 17 vol% as determined by X-ray diffraction analysis and optical metallography. The thermal diffusivity samples were 1.27-cm-diameter

disks with thicknesses of 0.133, 0.145, and 0.096 cm, respectively, for the 39, 26, and 17 vol% SiC compositions.

2.2. Specific Heat

The specific heat was measured with a Perkin–Elmer DSC-2 calorimeter [2]. This instrument was interfaced with an HP1000 minicomputer which controlled the DSC and performed all data reduction necessary for computation of the specific heat [2]. Two overlapping temperature scans were performed to cover the entire temperature range: 23–527°C for the low range and 427°C to the maximum temperature of $\approx$717°C for the high range. Temperature calibrations were performed by using the melting points of known standards and the temperature scale was adjusted to $\pm$0.5°C. The specific heat accuracy was checked with sapphire as an unknown and was within $\pm$3% of NBS values. This method is similar to that described by other authors [3–5].

2.3. Thermal Diffusivity

The thermal diffusivity was measured using the laser flash technique [6, 7]. The samples were measured under vacuum conditions from to 50 to 630°C. The thermal diffusivity was corrected for a finite laser pulse width and radiation loss from the sample faces [8]. Graphite references were checked before and after the sample runs and were within $\pm$5% of recommended values [9]. The sample temperature was measured using a thermocouple system which was calibrated to within $\pm$2°C.

2.4. Density

Sample density was calculated by using the measured sample dimensions and weight. Pieces were removed, sectioned, and examined by optical microscopy for observable voids. Observable porosity was estimated to be approximately 5%, however, most of the voids were in the Al matrix which corresponded to 6–8% void fraction in the Al depending on the Al/SiC ratio. The measured density varied from 88 to 91% of the calculated theoretical density for the three compositions. The discrepancy in the density was assumed to result from porosity in the SiC particles. Table I lists the measured and calculated densities for the three cermet compositions and the calculated SiC porosity, which varied from 14 to 31%. These porosity values are in the range reported in the literature for commercial SiC [10]. The sample densities and diffusivity values were corrected for thermal expansion effects, which were less than 1.1% [1].

Table I. Porosity Estimate of SiC Based on Measured Cermet Density and Theoretical Densities for SiC = 3.24 g · cm^{-3} and Al = 2.71 g · cm^{-3}

Vol% SiC (%)	Cermet theoretical density (g · cm^{-3})	Cermet measured density (g · cm^{-3})	Cermet porosity (%)	Aluminum porosity (%)	SiC porosity (%)
39	2.92	2.57	12	8	17
26	2.85	2.58	9	7	14
17	2.80	2.48	11	6	31

3. RESULTS AND DISCUSSION

3.1. Thermal Diffusivity

The diffusivity samples were initially baked at 135°C to remove any residues from the etching process used to remove the copper substrate. However, significant changes were measured in the diffusivity after three initial scans to 630°C. The initial diffusivity was almost 35% lower than the two subsequent runs, which agreed quite well with each other. This increase in diffusivity was probably due to a reduction in the contact resistance caused by sintering of granular regions of aluminum layed down during the plasma spray process. Based on these results, all further measurements on the remaining samples were performed after an initial high-temperature bakeout at 650°C in order to provide a stable microstructure. Figure 1 shows the diffusivity values obtained for the three cermet compositions, which, generally, decreased gradually with increasing temperature, then dropped more rapidly starting in the 520–590°C range. The maximum temperature was kept below the aluminum melt point of 660°C.

3.2. Specific Heat

The specific heat samples were also initially baked at 137°C to remove chemical residues. However, during an initial scan to 527°C, the 39 vol% SiC sample underwent an exothermic reaction centered at 227°C, possibly due to reaction of trapped residue. Repeat scans on the same sample did not show this exothermic activity; therefore, all subsequent samples were measured after a high-temperature bakeout at 527°C. Figure 1 shows the results of the initial DSC measurements after the bakeout on the three cermet compositions. Above 550°C the cermets started a melt transition well

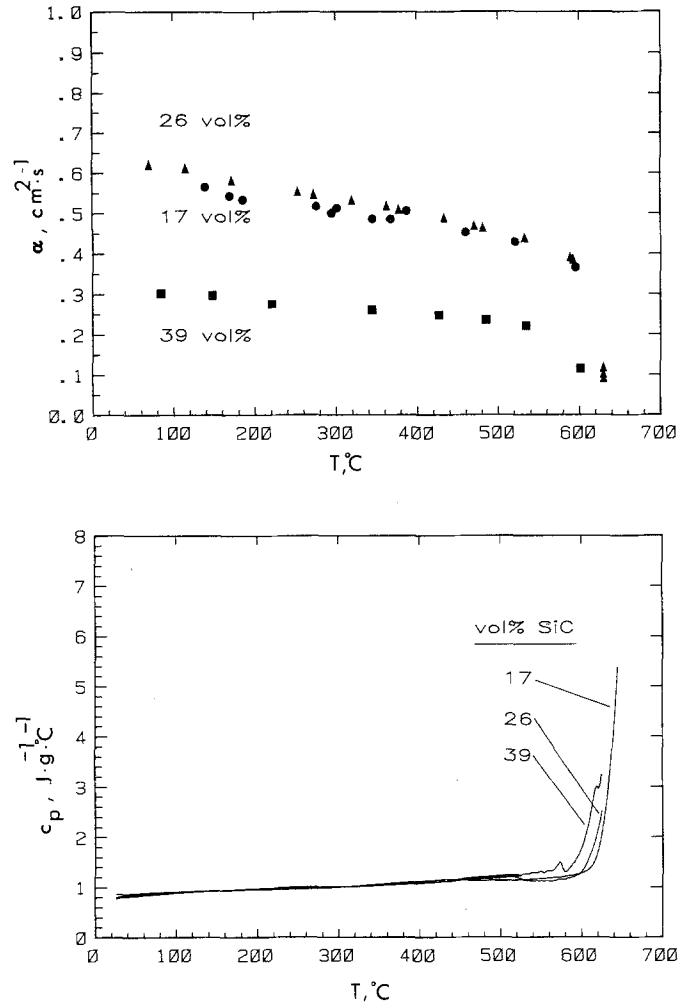

Fig. 1. (Upper) Thermal diffusivity of cermets with 17, 26, and 39 vol% SiC. Samples preheated at 650°C. (Lower) Specific heat of cermets with 17, 26, and 39 vol% SiC. Samples preheated at 527°C.

before the melting point of pure aluminum at 660°C. The onset of this melt regime shifted to a lower temperature as the volume fraction of SiC increased. The sample with the highest fraction of SiC, 39 vol%, showed two smaller endothermic transitions, near 570 and 610°C, superimposed on the larger endotherm.

The suppression of the melt transition and, especially, the 570°C endotherm for the 39 vol% SiC indicated that the aluminum matrix had

alloyed with silicon. The Al/Si binary system has a eutectic melt temperature of 577°C for Al/Si compositions with greater than 1.65 wt% Si [11]. To investigate this effect further, a sample of the 39 vol% SiC cermet was measured in the DSC from 500 to 720°C. Three temperature scans were made on the sample as shown in Fig. 2. Also shown in Fig. 2 for reference are the results of the measurement of a pure aluminum plasma-sprayed coating. The pure aluminum showed a melt temperature of 658°C with a slight amount of premelting, possibly due to impurities. The cermet measurements showed an initial melt endotherm in the 570–575°C range, as seen earlier, with a larger endothermic region rising to a peak in the 640–650°C range. The width of this transition region corresponds to the width of the two-phase region between the eutectic and the liquids [11]. The magnitude of the eutectic endotherm shown in Fig. 2 increased from scan 1 to scan 3 as more of the aluminum in this two-phase region melted. A sharp drop in the specific heat occurred when the liquids temperature was reached, at which temperature all of the aluminum was molten. The first scan had an endothermic peak at 651°C, while the next two scans peaked at 646 and 640°C, respectively. This downward shift could result from an increase in the percentage of silicon in the aluminum matrix since the liquids temperature decreases with increasing silicon content. It is postulated that after the cermet sample was taken into the molten state,

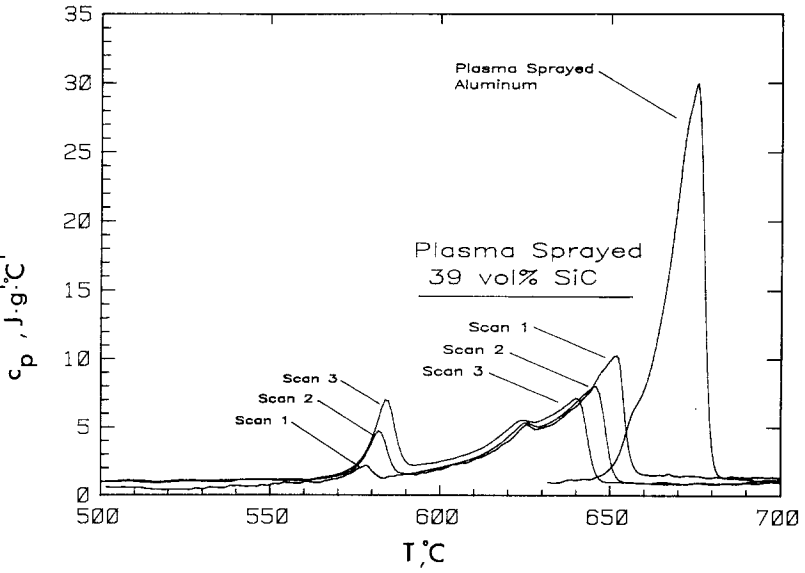

Fig. 2. Specific heat of 39 vol% SiC cermet and pure Al plasma-sprayed coating. Three successive measurements of the cermet are shown.

free silicon that had been contained in the SiC particles was able to diffuse into the molten aluminum. For the subsequent scans, the sample had experienced greater periods of time in the molten state during which the silicon content in the aluminum steadily increased. This postulated diffusion process is further indicated in Fig. 2 by the increasing magnitude of the eutectic melt endotherm near 577°C for each scan. As the silicon content increased, the fractional amount of the molten phase at the eutectic temperature increased as given by the inverse lever arm rule, thus increasing the magnitude of the melting endotherm.

A further check of this postulated increase in Si content was made by comparing the estimated liquidus temperature and estimated silicon weight percentage for the three successive scans with the liquids line of the phase diagram. The liquidus temperature was estimated as the temperature at the upper peak in the endothermic transition. The silicon weight percentage in the aluminum matrix was estimated by using the inverse lever arm rule and the estimated weight fractions of the molten- and solid-phase aluminum at the eutectic temperature.

The weight fraction of the eutectic molten phase at the eutectic temperature was estimated from the ratio of the area under the eutectic endothermic peak to the area under the total melt endotherm. The area under the total endotherm peak corresponds to the heat of fusion of the Al phase. This calculation was checked by measuring the endotherm area for a pure Al plasma-sprayed coating, which agreed within 3% of the known Al heat of fusion. The area under the eutectic melt region also includes some contribution from noneutectic composition material since the transition occurs over a finite temperature interval. Thus the eutectic fractional weight is somewhat overestimated, which will also overestimate the silicon weight percent. Figure 3 shows these calculated values and the ideal liquids line. The data follow the slope of the liquidus line quite well but are offset by a constant of +0.6 wt% Si, as was expected from the estimation procedure. Thus, the Al/Si alloying process explains the observed cermet thermal behavior.

The first scans in the DSC of the 17 and 26 vol% SiC samples showed only single endothermic transitions with lowered melt temperatures of 625 and 605°C, respectively, which indicated Si compositions in the Al matrix below the maximum solubility limit of 1.65 wt% Si. However, the first scan of the 39 vol% SiC cermet in the DSC showed a eutectic melt transition near 570°C, thus indicating the presence of at least 1.65 wt% Si in the Al matrix in the initial plasma-sprayed material. Diffusion of free Si from the SiC probably occurred after the plasma spray deposition when the Al was still at an elevated temperature. Although the Si distribution was probably not uniform throughout the Al, electron microprobe analysis showed no

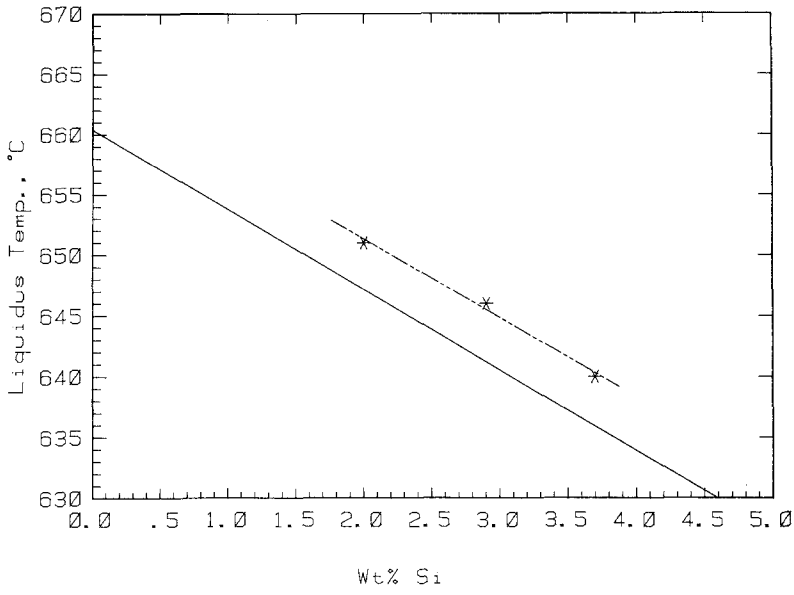

Fig. 3. Liquidus line for Al/Si alloy (solid line) and estimated liquidus temperature vs wt% Si for the 39 vol% SiC cermet (dashed line).

evidence of diffusion layers of Si in the Al at the Al/SiC interfaces within a resolution limit of 1 μm. To observe directly the initial state of the Al/SiC mix, a sample of the blended Al/SiC powder was measured in three successive scans in the DSC (see Fig. 4). The sample consisted of 20 vol% Al and 80 vol% SiC, which was used as the source material for the 39 vol% SiC coatings. The lower SiC content in the plasma-sprayed cermet resulted from SiC particle bounce at the cermet surface during the plasma spray procedure. The initial measurement on the powder showed only a melt transition at the Al melt point, thus indicating that no free Si was initially present in the Al powder. The second and third scans showed the eutectic melt transition at 577°C, with a broad endotherm continuing up to 640–650°C. The third scan showed a slight increase in the eutectic melt endotherm compared to the second scan. These results are similar to those obtained for the plasma-sprayed materials. However, the relative magnitude of the eutectic endotherm compared to the endotherm in the two-phase region was much greater in the powder than in the plasma-sprayed material, indicating as much as 4.5 wt% Si in the Al for the melted powder. This increase is due to the greater fraction of SiC present in the powder.

Inductively coupled plasma analysis for free Si was performed on the

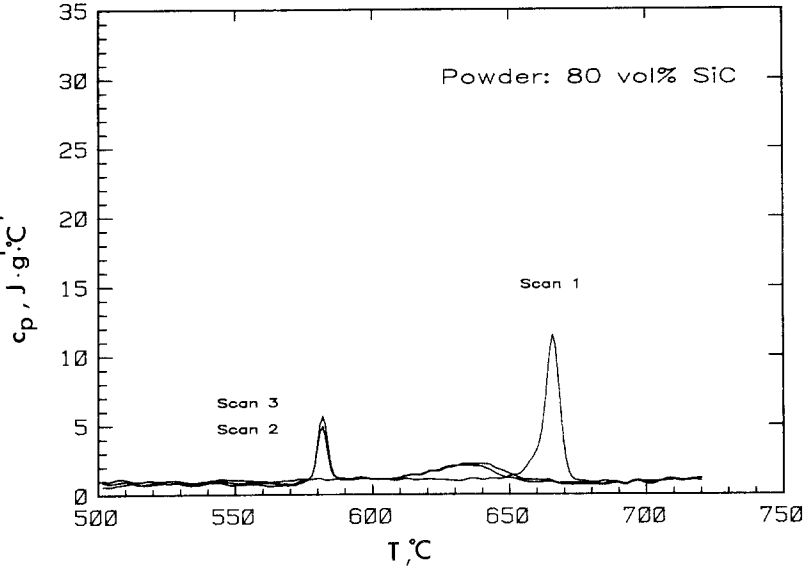

Fig. 4. Specific heat of 20 vol% Al/80 vol% SiC powder. Three successive scans are shown.

39 vol% SiC plasma-sprayed material as well as on the pure SiC powder. This analysis indicated a free Si content of 1.3 wt% the SiC powder. X-Ray diffraction analysis of the cermet indicated the presence of ≈ 2 vol% free Si with a grain size of ≈ 40 nm. These analyses substantiate the thermal analysis results.

3.3. Thermal Conductivity

The thermal conductivity was calculated using the thermal diffusivity and specific heat data shown in Fig. 1 and the measured densities listed in Table I. The accuracy limit for the thermal conductivity data is $\pm 10\%$ based on accuracy limits of $\pm 5\%$ for diffusivity, $\pm 3\%$ for specific heat, and $\pm 2\%$ for density. Figure 5 shows the results of these calculations. The thermal conductivity values for all three cermets were quite flat up to 500°C, above which they decreased slightly. The thermal conductivity values for the 17 and 26 vol% SiC samples agreed with each other within experimental errors over the temperature range 60–610°C. The thermal conductivity of the 39 vol% SiC sample over the same temperature range was $\approx 50\%$ lower than the conductivities of the other two compositions.

Effective medium theory was used to estimate the thermal conductivity of this two-component material, using literature values for the thermal con-

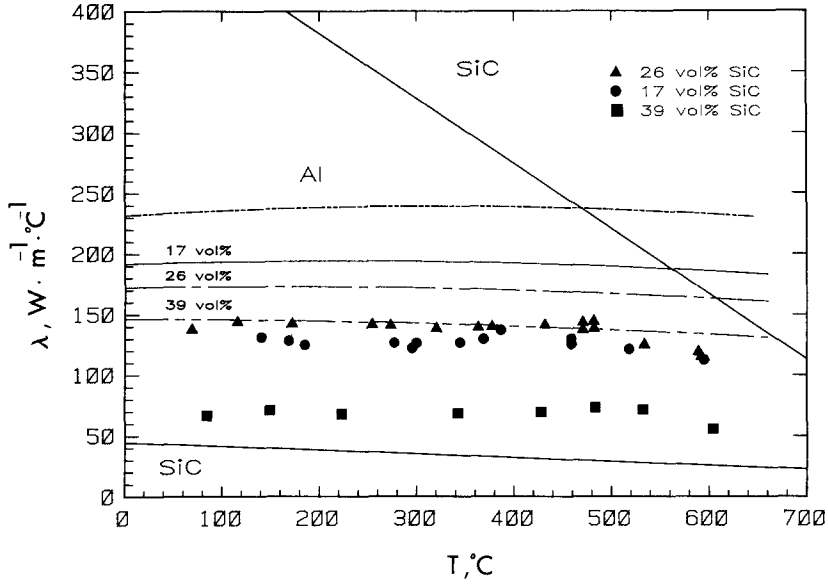

Fig. 5. Thermal conductivity of cermets with 17, 26, and 39 vol% SiC computed from measured specific heat, diffusivity, and density. Also shown are literature data for Al and SiC. SiC curves are for single-crystal and porous structures. Also shown are calculations of the effective conductivity using Maxwell's model and the literature values for Al and porous SiC.

ductivity of the Al and SiC in various models. Many analytical models exist for the calculation of the thermal conductivity of a two-phase medium [12]. The utility of a given model depends on how closely the assumptions about microstructure and component thermal properties match those of the real material. Fortunately, most analytical models agree very closely when the effective medium conductivity is not greatly different from the continuous phase conductivity, the discreet and continuous phase conductivities are not greatly different, and no significant discreet particle–particle contact occurs [12]. In this study, the cermets met these criteria with the ratio of the measured cermet conductivity to the Al matrix conductivity in the range 0.24–0.58. Several models of both the flux law and the Ohm's law type were used to calculate the cermet conductivity and were in very close agreement over the entire temperature range. Maxwell's model was chosen for calculational simplicity [13]. Figure 5 shows the experimental data and curves obtained using this model for the three cermet compositions as well as curves for the literature values of the Al and SiC [14, 10]. Two curves are shown for the SiC thermal conductivity to represent the range in conductivity reported as a function of sample porosity. The upper curve

represents the values for a single crystal of SiC, while the lower curve is that for a sample having ≈22% porosity. Since the experimental data for the cermets do not show any significant temperature dependence, the SiC particles in the cermet probably have a conductivity like that of the porous SiC and not like that of single-crystal SiC. This conclusion is in agreement with the density calculations shown in Table I, where the SiC was calculated to be 14–31% porous. Therefore, the lower SiC curve was used for these calculations. The conductivity of the Al matrix used in the calculation was reduced to account for the ≈7% porosity seen from the micrographs. The reduction factor calculated from Maxwell's model was 10%. The results of these calculations shown in Fig. 5 are higher than the experimental data but have the same basic temperature dependence. The difference in magnitude probably results from defects in the Al, such as dislocations and vacancies, which would result from rapid cooling after the plasma spray deposition as well from impurity defects diffused from the SiC. In addition, oxidation of the Al probably resulted in dispersed oxide in the Al matrix and oxide formation at the Al splat boundaries, which would reduce the Al thermal conductivity.

Figure 5 shows that the 17 vol% SiC sample had a slightly lower thermal conductivity than the sample with 26 vol% SiC, which is in contrast to the prediction of the effective medium model. However, Table I shows that the density of the 17 vol% SiC sample was much lower than that of the other two compositions. If this lower density were due to excess porosity in the Al matrix and not in the SiC phase, the matrix conductivity would be reduced in comparison to that of the other two sample compositions so that the predicted thermal conductivities of the 17 and 26 vol% SiC samples would be very similar.

Figure 5 also shows a slight decrease in thermal conductivity for all three compositions above ≈550°C. This decrease in measured conductivity at the highest temperature probably results from the formation of the molten Al phase above the eutectic temperature, which has a much lower thermal conductivity than the solid phase [14].

4. SUMMARY

The thermal properties of the plasma-sprayed Al/SiC cermets were affected by the presence of free Si in the SiC source material. The Si was able to diffuse from the SiC into the Al during plasma spray deposition and later during measurement. The diffusion of Si into the Al resulted in a eutectic phase with a ≈100°C lowered melting point that could degrade the performance of the cermet during actual use in a fusion device.

Modeling of the thermal conductivity tends to indicate that the cermet consisted of a defected Al matrix and porous, low-conductivity SiC particles.

ACKNOWLEDGMENTS

This work was supported by the U.S. Department of Energy, under Contrat DE-AC04-76DP00789. The authors express their gratitude to W. D. Drotning for this measurement of the thermal expansion and to A. J. Anaya for the measurement of the thermal diffusivity.

REFERENCES

1. M. F. Smith, J. B. Whitley, and J. M. McDonald, *Thin Solid Films* **118**:23 (1984).
2. Reference to a particular product or company implies neither a recommendation nor an endorsement by Sandia National Laboratories or the U.S. Department of Energy, nor a lack of suitable substitutes.
3. W. P. Brennan and A. P. Gray, *Thermal Analysis Application Study No. 9* (Perkin–Elmer Instrument Division, Norwalk, Conn., 1973).
4. S. C. Mraw and D. F. Naas, *J. Chem. Thermodyn.* **11**:567 (1979).
5. A. Fransson and G. Bäckström, *Int. J. Thermophys.* **6**:165 (1985).
6. W. J. Parker, R. J. Jenkins, et al., Navy Technical Report USNRDL-TR-424 (1960).
7. R. E. Taylor, *High Temp. High Press.* **11**:213 (1979).
8. J. A. Koski, in *Proceedings, Eighth Symposium on Thermophysical Properties, Vol. II. Thermophysical Properties of Solids and of Selected Fluids for Energy Transfer* (ASME, New York, 1982), p. 94.
9. E. Fitzer, *AGARD-R-606* (Technical Editing and Reproduction Ltd., Harford House, 7–9 Charlotte St., London WIP 1HD, 1973).
10. Y. S. Touloukian, R. W. Powell, C. Y. Ho, and P. G. Klemens, *Thermophysical Properties of Matter*, TPRC Data Series, Vol. 2 (IFI Plenum, New York–Washington, D.C., 1970), p. 585.
11. *Metals Handbook, Vol. 8*, 8th ed., T: Lyman, ed. (American Society for Metals, Metals Park, Ohio, 1973) p. 263.
12. R. A. Crane, R. I. Vachon, and M. S. Khader, in *Proceedings, Seventh Symposium on Thermophysical Properties* (ASME, New York, 1977), p. 109.
13. J. C. Maxwell, *A Treatise on Electricity and Magnetism, Vol. 1*, 3rd ed. (Oxford University Press, London, 1892), p. 440.
14. Y. S. Touloukian, R. W. Powell, C. Y. Ho, and P. G. Klemens, *Thermophysical Properties of Matter*, TPRC Data Series, Vol. 1 (IFI/Plenum, New York-Washington, D. C., 1970), p. 1.